Role of the [2Fe−2S] Cluster in Recombinant *Escherichia coli* Biotin Synthase†

Guy N. L. Jameson,‡ Michele Mader Cosper,§ Heather L. Hernández,§ Michael K. Johnson,*,§ and Boi Hanh Huynh*,‡

Department of Physics, Emory University, Atlanta, Georgia 30322, and Department of Chemistry and Center for Metalloenzyme Studies, University of Georgia, Athens, Georgia 30602

Received September 15, 2003; Revised Manuscript Received November 21, 2003

ABSTRACT: Biotin synthase (BioB) converts dethiobiotin into biotin by inserting a sulfur atom between C6 and C9 of dethiobiotin in an *S*-adenosylmethionine (SAM)-dependent reaction. The as-purified recombinant BioB from *Escherichia coli* is a homodimeric molecule containing one $[2Fe-2S]^{2+}$ cluster per monomer. It is inactive in vitro without the addition of exogenous Fe. Anaerobic reconstitution of the as-purified [2Fe−2S]-containing BioB with Fe^{2+} and S^{2-} produces a form of BioB that contains approximately one $[2Fe-2S]^{2+}$ and one $[4Fe-4S]^{2+}$ cluster per monomer ([2Fe−2S]/[4Fe−4S] BioB). In the absence of added Fe, the [2Fe−2S]/[4Fe−4S] BioB is active and can produce up to approximately 0.7 equiv of biotin per monomer. To better define the roles of the Fe−S clusters in the BioB reaction, Mössbauer and electron paramagnetic resonance (EPR) spectroscopy have been used to monitor the states of the Fe−S clusters during the conversion of dethiobiotin to biotin. The results show that the $[4Fe-4S]^{2+}$ cluster is stable during the reaction and present in the SAM-bound form, supporting the current consensus that the functional role of the [4Fe−4S] cluster is to bind SAM and facilitate the reductive cleavage of SAM to generate the catalytically essential 5′-deoxyadenosyl radical. The results also demonstrate that approximately $^2/_3$ of the [2Fe−2S] clusters are degraded by the end of the turnover experiment (24 h at 25 °C). A transient species with spectroscopic properties consistent with a $[2Fe-2S]^{+}$ cluster is observed during turnover, suggesting that the degradation of the $[2Fe-2S]^{2+}$ cluster is initiated by reduction of the cluster. This observed degradation of the [2Fe−2S] cluster during biotin formation is consistent with the proposed sacrificial S-donating function of the [2Fe−2S] cluster put forth by Jarrett and co-workers (Ugulava et al. (2001) *Biochemistry 40*, 8352−8358). Interestingly, degradation of the $[2Fe-2S]^{2+}$ cluster was found not to parallel biotin formation. The initial decay rate of the $[2Fe-2S]^{2+}$ cluster is about 1 order of magnitude faster than the initial formation rate of biotin, indicating that if the [2Fe−2S] cluster is the immediate S donor for biotin synthesis, insertion of S into dethiobiotin would not be the rate-limiting step. Alternatively, the [2Fe−2S] cluster may not be the immediate S donor. Instead, degradation of the [2Fe−2S] cluster may generate a protein-bound polysulfide or persulfide that serves as the immediate S donor for biotin production.

The ultimate step in the biosynthetic pathway of biotin involves the insertion of sulfur into dethiobiotin (DTB)[1] at the C6 and C9 positions with the loss of two hydrogen atoms. This reaction is catalyzed by the *bioB* gene product, termed biotin synthase or BioB, in a *S*-adenosyl-L-methionine (SAM)-dependent reaction (Scheme 1). The as-purified recombinant BioB from *Escherichia coli* is a homodimeric molecule of 78 kDa containing one $[2Fe-2S]^{2+}$ cluster per monomer (*1*−*4*). The presence of $[2Fe-2S]^{2+}$ clusters has also been reported in the as-purified recombinant BioBs from *Bacillus sphaericus* and *Arabidopsis thaliana* (*5*, *6*). However, the physiological relevance and functional roles of the [2Fe−2S] cluster have been the subjects of controversy ever since its identification, because spectroscopic and biochemical evidence accumulated so far (see preceding paper (*4*) and below) strongly implicate that BioB belongs to the "radical SAM" family of Fe−S enzymes (*7*), which utilize a [4Fe−4S] cluster (not a [2Fe−2S] cluster) to mediate reductive cleavage of SAM to generate a 5′-deoxyadenosyl radical as the catalytically essential oxidant.

Direct evidence for the involvement of adenosyl radicals in the activation and breaking of the two C−H bonds at the 6 and 9 positions of DTB has come from mass spectrometry studies of the BioB reaction, which showed transfer of deuterium from the deuterated substrate DTB, labeled at the C6 or C9 position or both, to the product deoxyadenosine (*8*). The obligatory SAM dependence of the biotin synthase reaction and the initial discovery that the $[2Fe-2S]^{2+}$ cluster in the as-purified enzyme can be converted quantitatively to $[4Fe-4S]^{2+}$ clusters using dithionite in the presence of 60%

† This work was supported by grants from the National Institutes of Health (Grant GM62542 to M.K.J., Grant GM47295 to B.H.H.) and a National Research Service Postdoctoral Fellowship (Grant DK 59730 to M.M.C.).

* To whom correspondence should be addressed. B.H.H.: telephone, 404-727-4295; fax, 404-727-0873; e-mail, vhuynh@emory.edu. M.K.J.: telephone, 706-542-9378; fax, 706-542-2353; e-mail, johnson@chem.uga.edu.

‡ Emory University.

§ University of Georgia.

[1] Abbreviations: BioB, gene product of *bioB* commonly referred to as biotin synthase; DTB, dethiobiotin; PLP, pyridoxal 5′-phosphate; SAM, *S*-adenosyl-L-methionine; DTT, dithiothreitol.

10.1021/bi035666v CCC: $27.50
Published on Web 01/30/2004

Scheme 1

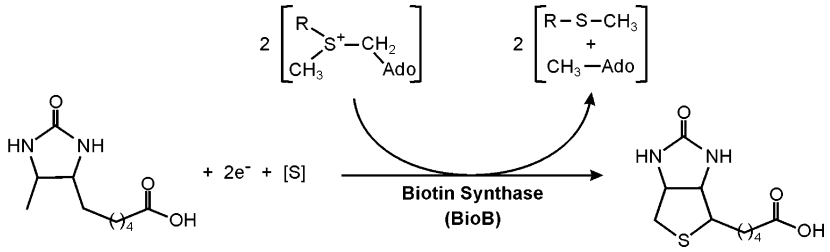

ethylene glycol or glycerol (*2*) led to the suggestion of a [4Fe−4S]-containing functional form of BioB. However, questions concerning the composition and type of Fe−S cluster in wild-type functional BioB were complicated by subsequent reports that showed that various forms of BioB, containing either exclusively [2Fe−2S] or [4Fe−4S] or a 1:1 mixture of [2Fe−2S] and [4Fe−4S] clusters, can be obtained under different reconstitution and experimental conditions (*3*, *9*−*11*). These observations have led to the proposal that BioB contains two distinct Fe−S cluster-binding sites with each site capable of binding either a [2Fe−2S] or a [4Fe−4S] cluster (*11*). Subsequently, it was shown by Mössbauer spectroscopy that the two clusters can be selectively labeled with ^{57}Fe, indicating the presence of distinct [2Fe−2S] and [4Fe−4S] binding sites in BioB (*12*). Taking into account the electrochemical properties obtained for these various forms of BioB and the expected redox potential in cells, Jarrett and co-workers (*11*) have proposed that the BioB form containing a 1:1 mixture of [2Fe−2S] and [4Fe−4S] clusters is the functional form of BioB in vivo. This form of BioB was also found to have maximal activity in vitro producing approximately 0.9 equiv of biotin per monomer in the absence of added Fe (*13*).

Single turnover experiments involving [2Fe−2S]/[4Fe−4S] BioB, which indicated the loss of the [2Fe−2S] cluster based on Fe and S analyses and UV/visible absorption changes, led Jarrett and co-workers to propose a mechanism in which the [4Fe−4S] cluster mediates the reductive cleavage of SAM and a bridging S of the [2Fe−2S] cluster serves as the immediate S donor for biotin (*13*). The [2Fe−2S] cluster is therefore destroyed by the end of the reaction. Degradation of the $[2Fe-2S]^{2+}$ cluster during turnover was demonstrated recently by a Mössbauer investigation of partially purified BioB (*14*). In contrast, BioB preparations containing mostly the [4Fe−4S] form of BioB were reported to have the capability of binding pyridoxal 5′-phosphate (PLP) and catalyzing desulfuration of cysteine by a mechanism similar to that used by the NifS and IscS enzymes (*15*). An alternative mechanism was therefore proposed, in which BioB possesses an intrinsic PLP-dependent cysteine desulfurase activity and the immediate S donor is a protein-bound persulfide generated via the intrinsic desulfurase reaction. Desulfurase-activity investigations of site-specific variants further suggest that the conserved cysteine residues Cys97 and Cys128 are the likely candidates for the persulfide binding site (*15*).

In the preceding paper, we have used a combination of UV/visible absorption, resonance Raman, and Mössbauer spectroscopies, coupled with analytical and activity measurements, to characterize the various Fe−S cluster-containing forms of recombinant *E. coli* BioB and to establish the transformations that can occur among these various forms of BioB (*4*). The results support the existence of distinct [4Fe−4S] and [2Fe−2S] binding sites in each BioB monomer. BioB contains six conserved cysteine residues, three of which are arranged in the CxxxCxxC (Cys53, Cys57, and Cys60) motif that is shared by all members of the radical SAM family to coordinate the catalytically active [4Fe−4S] cluster. Spectroscopic and reactivity studies of site-specific cysteine to alanine variants of BioB support coordination of these three cysteines to the [4Fe−4S] cluster (*16*, *17*). The remaining three conserved cysteine residues (Cys97, Cys128, and Cys188) were thus likely to be the ligands for the [2Fe−2S] cluster. Our results also showed that the BioB form containing a 1:1 ratio of [2Fe−2S] to [4Fe−4S] ([2Fe−2S]/[4Fe−4S] BioB) is the most active form in vitro without added Fe, in agreement with the finding of Ugulava et al. (*11*). Our data, however, provide no evidence to support PLP binding or PLP-dependent cysteine desulfurase activity for BioB.

In this manuscript, Mössbauer and electron paramagnetic resonance (EPR) spectroscopy have been used to monitor the Fe−S clusters in [2Fe−2S]/[4Fe−4S] BioB during catalytic turnover. The objectives were to obtain information to enhance our understanding of the BioB mechanism and to evaluate the proposed sacrificial S-donating function of the [2Fe−2S] cluster. The results show that during turnover the [4Fe−4S] cluster is stable and present in the SAM-bound $[4Fe-4S]^{2+}$ state, while the majority of the [2Fe−2S] cluster is destroyed, in general agreement with the conclusion made by Jarrett and co-workers (*13*) and with the Mössbauer results obtained for the partially purified BioB (*14*). However, in contrast to the UV/visible absorption studies, our data demonstrate that not all of the $[2Fe-2S]^{2+}$ clusters are destroyed and that degradation of the $[2Fe-2S]^{2+}$ cluster proceeds via a $[2Fe-2S]^{+}$ intermediate and does not parallel the production of biotin during turnover. Implications of these observations on the possible functional roles of the [2Fe−2S] cluster and on the BioB mechanism are presented.

MATERIALS AND METHODS

Materials. Chemicals were purchased from Sigma-Aldrich or Fisher, unless otherwise stated. ^{57}Fe-enriched metal nuggets (95.4% enrichment) were purchased from WEB Research. ^{57}Fe-enriched ferric ammonium citrate and $Fe^{II}SO_4$ was prepared by a literature method (*18*). The plasmid pEE1010 containing the gene encoding *E. coli* flavodoxin reductase was a kind gift from Peter Reichard at the Karolinska Institute, and the *E. coli* strain DH01 overexpressing *E. coli* flavodoxin was a kind gift from Rowena Matthews at the University of Michigan. Anaerobic experiments were performed under an argon atmosphere in a Vacuum Atmospheres glovebox at oxygen levels <5 ppm.

E. coli BL21-gold[DE3] pT7-7ecbioB-1 was anaerobically cultivated, and *E. coli* wild-type (WT) [2Fe−2S] BioB was aerobically purified as previously described (*4*). *E. coli* WT [2Fe−2S]/[4Fe−4S] BioB was prepared by reconstitution of the as-purified [2Fe−2S] BioB by a previously published method (*4*, *13*). For Mössbauer studies, ^{57}Fe-enriched [2Fe−2S] BioB was purified from *E. coli* cells grown in ^{57}Fe-enriched medium and subsequently reconstituted with either natural Fe (2.2% ^{57}Fe) or ^{57}Fe (95.4% enrichment) to produce [2Fe−2S]/[4Fe−4S] BioB with either only the [2Fe−2S] cluster or both clusters labeled with ^{57}Fe.

Assay of Biotin Synthase Activity. The BioB assay was performed under strictly anaerobic conditions according to a procedure specified by Gibson and colleagues (*19*, *20*), with the following modifications. In 100 mM Tris-HCl (pH 8.0) buffer with 10 mM KCl, 200 μM *E. coli* WT [2Fe−2S]/[4Fe−4S] BioB was combined with 10 mM DTT, 2 mM cysteine, 10 mM fructose-1,6-biphosphate, 2 mM NADPH, 80 μM flavodoxin, 40 μM flavodoxin reductase, and 2 mM SAM. The reaction was commenced by the addition of 400 μM DTB, and the BioB reaction was allowed to proceed at 25 °C. At various time points, from 5 min to 24 h, samples were removed, placed in a Mössbauer cup or EPR tube, and immediately frozen in liquid N_2. EPR spectra of Mössbauer samples were recorded after the collection of the Mössbauer data was completed. In addition, a 50 μL aliquot was removed and added to 5 μL of saturated sodium acetate (pH 4.0), which resulted in the precipitation of protein. The protein was removed by centrifugation at 13 000 × *g* for 10 min, and the supernatant was analyzed for biotin using the *Lactobacillus plantarum* ATCC 8014 microbiological assay (*21*, *22*). The BioB assay was also performed using the conditions specified by Jarrett and co-workers (*13*).

Determination of Protein and Fe Concentrations. Protein concentrations were determined by the *DC* protein assay (Bio-Rad), using BSA as a standard. All protein concentrations for wild-type BioB were multiplied by the correction factor of 1.1 (*4*). Iron concentrations were determined using bathophenanthroline under reductive conditions after digestion of the protein in 0.8% $KMnO_4$/0.2 M HCl (*13*) as described by Fish (*23*). All sample concentrations are expressed per BioB monomer.

Spectroscopic Studies. UV−visible absorption spectra were recorded under anaerobic conditions in screw top 1 mm cuvettes using a Shimadzu UV-3101PC spectrophotometer. X-band (∼9.5 GHz) EPR spectra were recorded on a Bruker ESP-300E EPR spectrometer equipped with an ER-4116 dual-mode cavity and an Oxford Instrument ESR-9 flow cryostat. Resonances were quantified under nonsaturating conditions using a 1 mM CuEDTA standard. EPR spectra were simulated using the Bruker Simphonia and WinEPR software packages. Mössbauer spectra were recorded in a weak-field and a strong-field spectrometer described elsewhere (*24*). The zero velocity of the spectra refers to the centroid of the room-temperature spectrum of a metallic iron foil. Analysis of the Mössbauer data was performed with the program WMOSS (Web Research).

RESULTS

Mössbauer Results. [2Fe−2S]/[4Fe−4S] BioB with the [2Fe−2S] cluster selectively labeled with ^{57}Fe ([2^{57}Fe−2S]/[4Fe−4S] BioB) was prepared for single turnover experiments (see Materials and Methods). At reaction time points of 5 min, 45 min, and 24 h, samples were removed and frozen for Mössbauer investigations. Since Mössbauer spectroscopy can detect only ^{57}Fe, these measurements allowed us to selectively monitor changes to the [2Fe−2S] clusters during enzymatic turnover. To monitor changes occurring at both [2Fe−2S] and [4Fe−4S] clusters during turnover, proteins of [2Fe−2S]/[4Fe−4S] BioB with both clusters labeled with ^{57}Fe were also prepared, and samples were taken at reaction time points of 5 min, 45 min, 90 min, 3 h, 5 h, and 24 h for Mössbauer investigations. In an effort to correlate the Mössbauer observations, which provide information on the time evolution of the Fe−S clusters, with the production of biotin, samples were also removed at the same time points for biotin assay. The results are presented below.

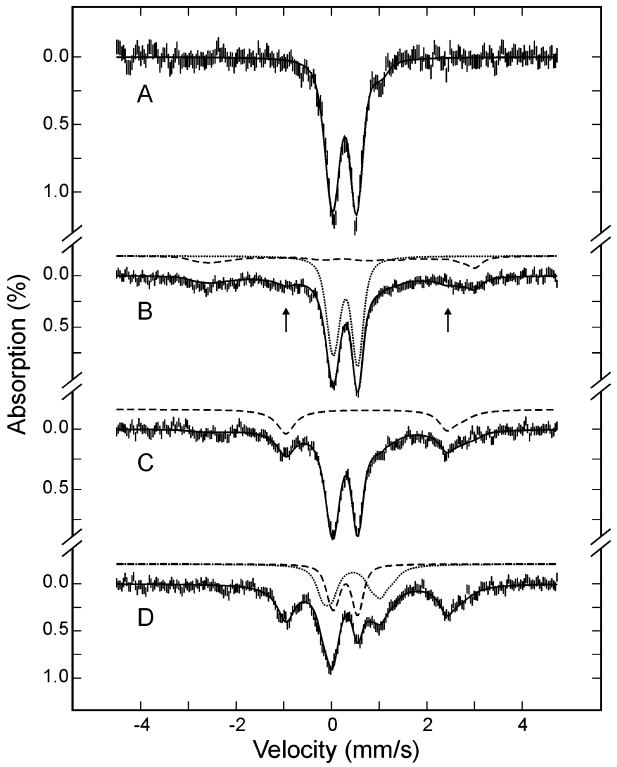

FIGURE 1: Mössbauer spectra (hatched marks) of as-prepared [2^{57}Fe−2S]/[4Fe−4S] BioB (A) and samples taken at 5 min (B), 45 min (C), and 24 h (D) reaction time points during the single turnover reaction of the enzyme. The data were recorded at 4.2 K in a field of 50 mT oriented parallel to the γ-beam. The solid lines overlaid with the experimental spectra are superpositions of theoretical spectra of the spectral components described in text and using the absorption percentages listed in Table 1. Also shown are some of the individual spectral components: $[2Fe-2S]^{2+}$, dotted line in panel B and dashed line in panel D; $[2Fe-2S]^{+}$, dashed line in panel B; SAM bound $[4Fe-4S]^{2+}$, dotted line in panel D; $Fe^{II}S_4$/N/O, dashed line in panel C. These spectral components are scaled to the percent absorption listed in Table 1. The two arrows in panel B indicate the positions of the doublet arising from the $Fe^{II}S_4$/N/O species.

[2^{57}Fe−2S]/[4Fe−4S] BioB. Figure 1A shows the Mössbauer spectrum (hatched marks) of the as-prepared [2^{57}Fe−2S]/[4Fe−4S] BioB recorded at 4.2 K in a magnetic field of 50 mT oriented parallel to the γ-beam. As expected, the spectrum is very similar to that of the [2^{57}Fe−2S]/[4Fe−4S] BioB reported in the preceding paper (*4*). It consists of a major quadrupole doublet representing the $[2Fe-2S]^{2+}$

cluster accounting for approximately 90% of the total Fe absorption and a minor doublet (∼10%) that may be assigned to a $[4Fe-4S]^{2+}$ cluster. The solid line overlaid with the experimental spectrum is a superposition of the two corresponding doublets reported in the preceding paper (*4*) with the percent absorptions mentioned above. In all of our [2Fe−2S]/[4Fe−4S] BioB preparations, we have consistently obtained an Fe stoichiometry of 4.3 to 4.4 Fe per BioB monomer, suggesting a constant cluster composition in our preparations. For the BioB preparation of this turnover experiment, protein and Fe determination also yield 4.4 Fe/BioB monomer. On the basis of this observation and the approximate 0.75:0.66 [2Fe−2S]/[4Fe−4S] cluster content obtained for our [2Fe−2S]/[4Fe−4S] BioB preparations (*4*), it is assumed that this preparation of BioB also contains approximately 0.75 [2Fe−2S] cluster per BioB monomer. In other words, it is assumed that 90% Fe absorption (percent absorption found for the [2Fe−2S] cluster) of these turnover samples corresponds to 0.75 [2Fe−2S] cluster/monomer (or 1.5 Fe/monomer).

Mössbauer Time Course for the Single Turnover of [2^{57}Fe−2S]/[4Fe−4S] BioB. Also shown in Figure 1 are the Mössbauer spectra (hatched marks) of samples taken at 5 min (B), 45 min (C), and 24 h (D) reaction time points during the single turnover reaction of [2^{57}Fe−2S]/[4Fe−4S] BioB. These spectra were recorded at 4.2 K in a parallel field of 50 mT. Detailed analysis of the data indicates that these spectra can be decomposed into four spectral components, details of which are presented in the following. The major spectral component observed in the spectrum of the 5-min sample (Figure 1B) is the central quadrupole doublet originating from the $[2Fe-2S]^{2+}$ cluster. Under turnover conditions, the parameters obtained for the $[2Fe-2S]^{2+}$ cluster ($\Delta E_Q = 0.51 \pm 0.03$ mm/s, $\delta = 0.29 \pm 0.02$ mm/s, half-width (left) = 0.29 mm/s, and half-width (right) = 0.27 mm/s) are within statistical errors similar to those obtained for the $[2Fe-2S]^{2+}$ cluster in the as-prepared [2Fe−2S]/[4Fe−4S] BioB (*4*). The dotted line displayed in Figure 1B is a quadrupole doublet simulated with the above parameters and scaled to 58% of the Fe absorption. In addition to this central doublet, the spectrum of the 5-min sample exhibits at least two more spectral components, one of which is a broad paramagnetic spectrum with absorption ranging from −3 mm/s to +3 mm/s. In accordance with the EPR measurement (see below), which shows the appearance of paramagnetic species after 5 min, this broad spectrum must be associated with the paramagnetic species detected in the EPR measurements. As presented below, the EPR data suggest two possible assignments, $S = {}^1/_2$ $[2Fe-2S]^+$ or $[4Fe-4S]^+$ clusters with the relaxation properties strongly favoring the $[2Fe-2S]^+$ cluster assignment. The total hyperfine splitting of this paramagnetic Mössbauer spectral component (∼6 mm/s) is too large for that of a typical $[4Fe-4S]^+$ cluster (∼4 mm/s) but is consistent with that of a $[2Fe-2S]^+$ cluster. To illustrate this point, a theoretical spectrum of the reduced parsley ferredoxin (*25*), a [2Fe−2S]-containing ferredoxin, is plotted on top of the experimental data as a dashed line (Figure 1B). To match the amplitude of the paramagnetic spectral component, the theoretical spectrum is scaled to 20% of the total Fe absorption, indicating that it represents approximately 0.2 $[2Fe-2S]^+$ cluster per monomer of BioB. This value is in good agreement with the spin quantitation of the corresponding EPR signal. Taken together, the EPR and Mössbauer evidence support the appearance of $[2Fe-2S]^+$ clusters at the beginning of the turnover reaction. Unfortunately, because of the substoichiometric accumulation of this species, the broad features of this paramagnetic component, and the limit on protein concentration that can be used for the turnover experiments (less than 200 μM in BioB monomer), it is impractical to obtain spectra with sufficient statistics that would allow us to determine the hyperfine parameters of this paramagnetic component.

The third spectral component is a broad quadrupole doublet, the positions of which are indicated by the two arrows shown in the 5-min spectrum (Figure 1B). The intensity of this component increases substantially and becomes more visible in the spectrum of the 45-min sample (Figure 1C), which can thus be used for the characterization of this component. In our analysis, we have used two equal-intensity overlapping quadrupole doublets to simulate the line shape of this broad quadrupole doublet, and the parameters obtained are $\Delta E_Q(1) = 3.36$ mm/s, $\delta(1) = 0.73$ mm/s, $\Delta E_Q(2) = 3.65$ mm/s, and $\delta(2) = 0.86$ mm/s. These parameters are typical for high-spin Fe^{II} compounds and the parameters for doublet 1 are characteristic of tetrahedral, sulfur-coordinated Fe^{II} compounds. The broad line shape suggests a distribution in the Fe coordination environment. This component is thus assigned to possible degradation products of the $[2Fe-2S]^{2+}$ cluster and is labeled as $Fe^{II}S_4$/N/O. For illustration, a theoretical simulation of this component is plotted as a dashed line in Figure 2C and is scaled to 25% of the total Fe absorption. Similar $Fe^{II}S_4$/N/O species have also been observed as minor components in reconstituted BioB and have been assigned as impurities (*10*, *12*).

The fourth spectral component detected in this turnover study is another quadrupole doublet that can be assigned to a SAM-bound $[4Fe-4S]^{2+}$ cluster. The presence of this component is most obvious in the spectrum of the 24 h sample (Figure 1D). To illustrate the presence of such a component, a theoretical spectrum of the SAM-bound [4Fe−4S] cluster in BioB (*26*) is plotted in Figure 1D as a dotted line and scaled to 38% of the total Fe absorption. Using these four spectral components, namely, the $[2Fe-2S]^{2+}$, $[2Fe-2S]^+$, $Fe^{II}S_4$/N/O, and SAM-bound $[4Fe-4S]^{2+}$ components, we are able to reproduce the three reaction-time dependent spectra shown in Figure 1B−D. The solid lines overlaid with the experimental data are superpositions of these four spectral components with the absorption percentages listed in Table 1. With the above-mentioned assumption that 90% of the Fe absorption corresponds to 1.5 Fe/BioB monomer, it is possible to convert the observed time-dependent percentages of these four components into equivalents per monomer (listed in Table 1) and thus provide information about the time evolution of these four Fe species. The results indicate that under the turnover conditions, within the first 5 min, the $[2Fe-2S]^{2+}$ cluster is partially reduced to the $[2Fe-2S]^+$ state and partially degraded to the mononuclear $Fe^{II}S_4$/N/O species. Degradation of the $[2Fe-2S]^{2+}$ cluster most likely occurs via the reduced $[2Fe-2S]^+$ state, since the reduced cluster appears to be a transient state based on both Mössbauer and EPR studies (see below). At 45 min, a substantial number of the $[2Fe-2S]^{2+}$ clusters have disintegrated and more $Fe^{II}S_4$/N/O species are observed. However, the increased amount of $Fe^{II}S_4$/N/O cannot account for all

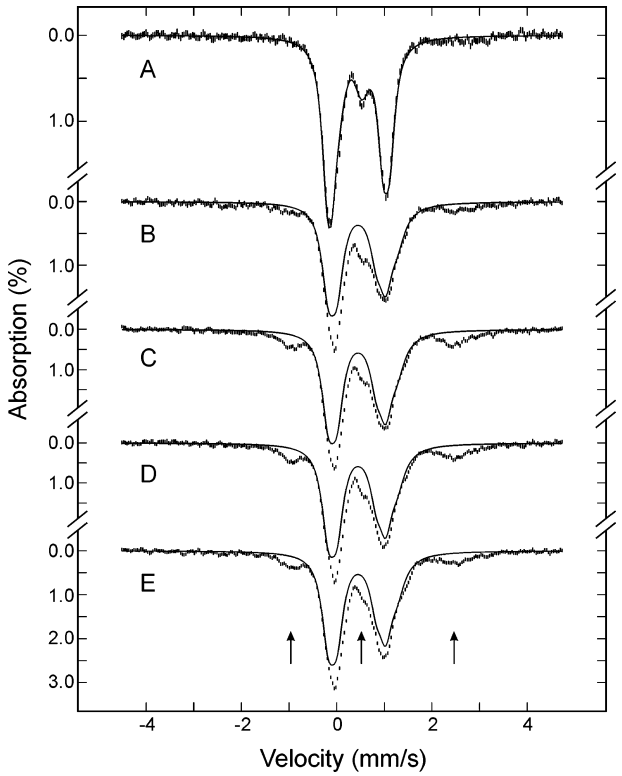

FIGURE 2: Time-dependent Mössbauer spectra (hatched marks) of ^{57}Fe-enriched [2Fe−2S]/[4Fe−4S] BioB during single turnover. Samples were taken at 0 (A), 5 min (B), 45 min (C), 3 h (D), and 24 h (E) reaction time points during turnover and the spectra were recorded at 4.2 K in a field of 50 mT oriented parallel to the γ-beam. The solid line in panel A is the superposition of theoretical spectra of the $[2Fe-2S]^{2+}$ and $[4Fe-4S]^{2+}$ cluster simulated with parameters reported in the preceding paper (*4*) and percent absorptions mentioned in text. The solid lines shown in panels B−E are simulated theoretical spectra of the SAM-bound $[4Fe-4S]^{2+}$ cluster (*26*) and are scaled to 76% of the total absorptions. The central arrow in panel E indicates the position of the high-energy line of the quadrupole doublet of the $[2Fe-2S]^{2+}$ cluster, and the other two arrows indicate the positions of the broad quadrupole doublet of the $Fe^{II}S_4$/N/O species.

the Fe released from the degraded $[2Fe-2S]^{2+}$ clusters, and interestingly, additional $[4Fe-4S]^{2+}$ clusters (SAM-bound) are formed. The degradation of the $[2Fe-2S]^{2+}$ cluster and formation of the $[4Fe-4S]^{2+}$ cluster were observed to continue with reaction time, and by 24 h, approximately 50% of the Fe released through the degradation of the [2Fe−2S] cluster is reassembled as [4Fe−4S] clusters. Conversion of [2Fe−2S] clusters to [4Fe−4S] clusters in BioB under anaerobic conditions has been observed previously (*2*, *9*), but has not been reported under turnover conditions. Our inability to assemble a $[4Fe-4S]^{2+}$ cluster at the [2Fe−2S] binding site (*4*), coupled with the fact that the assembled [4Fe−4S] cluster appears in the SAM-bound form, indicates that the [4Fe−4S] cluster is assembled at the [4Fe−4S] binding site. With the limited number of available time points, it is not possible to formulate a mechanistic model to describe this cluster disintegration and reassembly process observed here. A possible scenario would be for the Fe to be released into solution through degradation of the [2Fe−2S] cluster and then reassembled at unoccupied [4Fe−4S] binding sites. The appearance of the $Fe^{II}S_4$/N/O species prior to the assembly of the [4Fe−4S] cluster supports such a scenario.

Mössbauer Time Course for the Single Turnover of ^{57}Fe-enriched [2Fe−2S]/[4Fe−4S] BioB. Figure 2 shows the Mössbauer spectra (hatched marks) of the as-prepared ^{57}Fe-enriched [2Fe−2S]/[4Fe−4S] BioB (A) and of samples taken at various time points (B−E) during a single turnover reaction of the ^{57}Fe-enriched enzyme. The data were recorded at 4.2 K in a parallel field of 50 mT. Similar to the spectrum of the [2Fe−2S]/[4Fe−4S] BioB reported in the preceding paper (*4*), the as-prepared [2Fe−2S]/[4Fe−4S] BioB for the turnover experiment also exhibits two quadrupole doublets representing the $[2Fe-2S]^{2+}$ and the $[4Fe-4S]^{2+}$ clusters. The parameters of these two doublets are identical to those reported previously (*4*), but the absorption ratio of these two doublets of the turnover preparation, 18:82 [2Fe−2S]/[4Fe−4S], is different from that of the preceding paper (36:64 [2Fe−2S]/[4Fe−4S]) (*4*). This observation could be rationalized by a lower than normal population of [2Fe−2S] cluster in the turnover preparation. However, this preparation of BioB has a metal content (4.4 Fe/BioB monomer), UV−visible absorption properties, EPR properties (see below), and biotin synthase activity (see below) that are comparable to those of our other [2Fe−2S]/[4Fe−4S] BioB preparations. It is therefore likely that this preparation of BioB contains a cluster composition that is similar to the other preparations (i.e., ∼0.72−0.75 [2Fe−2S] and ∼0.66−0.72 [4Fe−4S] clusters per monomer). Since the ^{57}Fe-enriched [2Fe−2S]/[4Fe−4S] BioB was prepared by reconstituting a [4Fe−4S] cluster onto the [2Fe−2S] BioB isolated from cells grown in ^{57}Fe-enriched medium, the lower than expected Mössbauer absorption for the $[2Fe-2S]^{2+}$ cluster may reflect an inefficient ^{57}Fe enrichment of the [2Fe−2S] cluster during cell growth. Unfortunately, it is not possible to distinguish between these two possibilities, and this ambiguity does introduce an uncertainty into our interpretation of the time-dependent Mössbauer data presented next. On the basis of the above-mentioned chemical, spectroscopic, and biochemical evidence, we have assumed the latter possibility for the interpretation of the Mössbauer time course data. Despite the above-noted ambiguity, the data do provide definitive information on the state of the [4Fe−4S] cluster during turnover, which cannot be obtained with the [2^{57}Fe−2S]/[4Fe−4S] BioB, and the assumed [2Fe−2S] content does yield time-dependent information about the [2Fe−2S] cluster that is in good agreement with results obtained from the [2^{57}Fe−2S]/[4Fe−4S] BioB turnover study.

At first glance, the time-dependent Mössbauer spectra (hatched marks) taken during the single turnover of the ^{57}Fe-enriched [2Fe−2S]/[4Fe−4S] BioB (Figure 2, B−E) appear to show little time variation. Since the major Fe absorption in these samples arises from the [4Fe−4S] cluster (∼80%), the lack of major changes in these spectra indicates that the state of the [4Fe−4S] cluster remains constant throughout these time points. Furthermore, a comparison of the turnover spectra with a previously reported theoretical spectrum of a SAM-bound $[4Fe-4S]^{2+}$ cluster in BioB (*26*) indicates that under turnover conditions, the majority of the [4Fe−4S] clusters is present in the SAM-bound $[4Fe-4S]^{2+}$ form; the SAM-bound $[4Fe-4S]^{2+}$ spectrum is plotted as solid lines in Figure 2B−E and scaled to 76% of the total Fe absorption of each experimental spectrum. Consequently, the time variation observed for these spectra is mainly due to changes occurring at the $[2Fe-2S]^{2+}$ cluster. The main features that

Table 1: Mössbauer Percent Absorption and Quantification of ^{57}Fe Species Detected in [2^{57}Fe−2S]/[4Fe−4S] BioB during Single Turnover

	percent absorption (clusters/monomer)				
reaction time	$[2Fe-2S]^{2+}$	$[2Fe-2S]^{+}$	$[4Fe-4S]^{2+}$	SAM−$[4Fe-4S]^{2+}$	$Fe^{II}S_4$/N/O
0	90 ± 3 (0.75 ± 0.03)		10 ± 2 (0.04 ± 0.01)		
5 min	58 ± 3 (0.48 ± 0.03)	∼20 (∼0.17)		7 ± 2 (0.03 ± 0.01)	6 ± 2
45 min	53 ± 3 (0.44 ± 0.03)	∼10 (∼0.08)		16 ± 3 (0.07 ± 0.01)	25 ± 3
24 h	25 ± 3 (0.21 ± 0.03)			38 ± 3 (0.16 ± 0.01)	36 ± 3

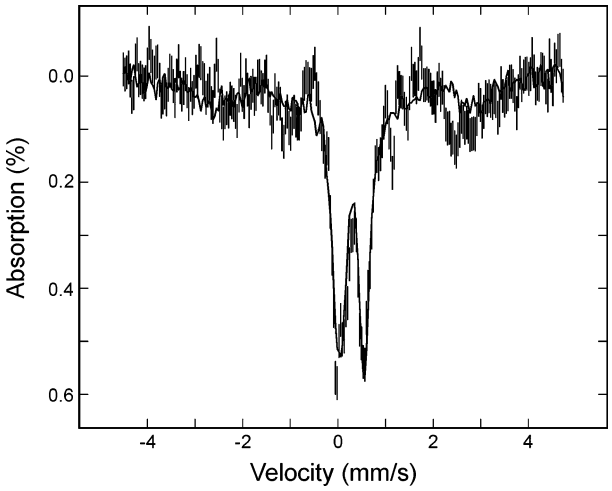

FIGURE 3: Mössbauer spectrum (hatched marks) prepared from the spectrum shown in Figure 2A by removing the contribution of the SAM-bound $[4Fe-4S]^{2+}$ cluster. This prepared spectrum compares well with that of the 5-min sample (solid line) during turnover of the [2^{57}Fe−2S]/[4Fe−4S] BioB shown in Figure 1B.

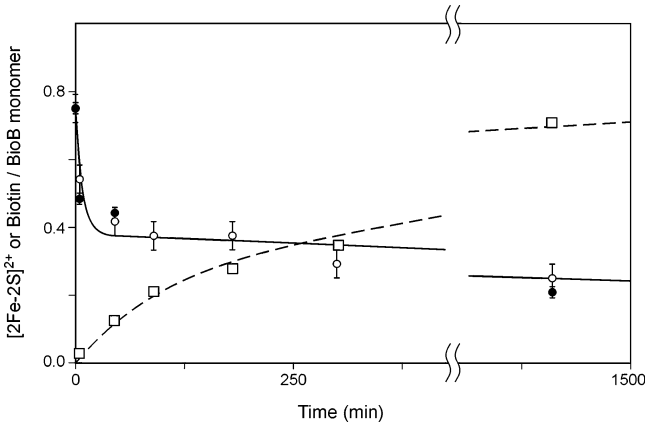

FIGURE 4: $[2Fe-2S]^{2+}$ cluster degradation (circles) and biotin production (squares) during BioB single turnover. The filled circles are data obtained from the [2^{57}Fe−2S]/[4Fe−4S] BioB turnover, and the empty circles are from the ^{57}Fe-enriched [2Fe−2S]/[4Fe−4S] BioB turnover. The solid and dashed lines are simulations of the $[2Fe-2S]^{2+}$ decay and biotin production, respectively, as described in text.

can be seen to change with time are (1) a decrease in intensity of the high-energy line of the $[2Fe-2S]^{2+}$ doublet (marked by a central arrow) and (2) an increase in intensity of the $Fe^{II}S_4$/N/O doublet (marked by two arrows at the sides). These changes are consistent with those observed for the turnover of the [2^{57}Fe−2S]/[4Fe−4S] BioB and indicate degradation of the [2Fe−2S] cluster during turnover. To demonstrate that quantitative information about the time evolution of the [2Fe−2S] cluster can be obtained from these spectra, despite the fact that the major contribution to these spectra is from the SAM-bound $[4Fe-4S]^{2+}$ cluster, we have removed the [4Fe−4S] contribution from the 5-min turnover spectrum and plotted the resulting spectrum in Figure 3 (hatched marks) and compared it with the 5-min turnover spectrum of the [2^{57}Fe−2S]/[4Fe−4S] BioB (solid line). It can be seen that the central quadrupole doublets representing the [2Fe−2S] cluster in these two spectra are very similar and the high-energy line is practically identical. Consequently, it is possible to use the $[2Fe-2S]^{2+}$ doublet (described in the preceding section) to estimate the percent absorption of the $[2Fe-2S]^{2+}$ cluster in the ^{57}Fe-enriched $[2Fe-2S]^{2+}$/$[4Fe-4S]^{2+}$ BioB samples during turnover. The results obtained are 13%, 10%, 9%, 9%, 7%, and 6% for the 5-min, 45-min, 90-min, 3-h, 5-h, and 24-h sample, respectively. Assuming the starting material contains 0.75 $[2Fe-2S]^{2+}$ cluster per BioB monomer (see above), these estimated percent absorptions can be converted into equivalents of clusters, and the results are plotted in Figure 4 (opened circles).

Degradation of the $[2Fe-2S]^{2+}$ Cluster Does Not Parallel the Production of Biotin During Turnover. As presented above, the Mössbauer data provide a quantitative measure of the time evolution of the $[2Fe-2S]^{2+}$ cluster in BioB during turnover. Figure 4 displays the data obtained from both turnover experiments with the [2^{57}Fe−2S]/[4Fe−4S] BioB (filled circles) and the ^{57}Fe-enriched $[2Fe-2S]^{2+}$/$[4Fe-4S]^{2+}$ BioB (opened circles). Within experimental uncertainty, both sets of data are in very good agreement and show a rapid disappearance of the $[2Fe-2S]^{2+}$ clusters within the first 45 min followed by a much slower decay of the cluster. After 24 h, approximately one-third of the clusters (∼0.25 $[2Fe-2S]^{2+}$/monomer) remain intact. This biphasic behavior cannot be described by a simple single exponential decay, and probably reflects a complex degradation process. With the limited time points available, it is neither possible nor desirable to attempt to deduce a mechanistic model for this apparently complex decay of the $[2Fe-2S]^{2+}$ cluster. However, the data are sufficient, both in number and accuracy, for examining whether the decay of the $[2Fe-2S]^{2+}$ cluster during turnover can be correlated with the production of biotin. For such a purpose, we have simulated the time evolution of the $[2Fe-2S]^{2+}$ cluster, $A(t)$, as an addition of two exponential decays (eq 1).

$$A(t) = A_1 \exp(-k_1 t) + A_2 \exp(-k_2 t) \qquad (1)$$

The solid line plotted in Figure 4 is a theoretical curve of eq 1 with $A_1 = 0.37$ clusters/monomer, $A_2 = 0.38$ clusters/monomer, $k_1 = 0.13$ min^{-1}, and $k_2 = 0.0003$ min^{-1}. In this simulation, we have assumed that the sum of A_1 and A_2 is 0.75 clusters/monomer. It should be emphasized that this approach is only to provide a quantitative simulation of the time course of the decay of the $[2Fe-2S]^{2+}$ cluster for the purpose of comparison with the production of biotin, to be

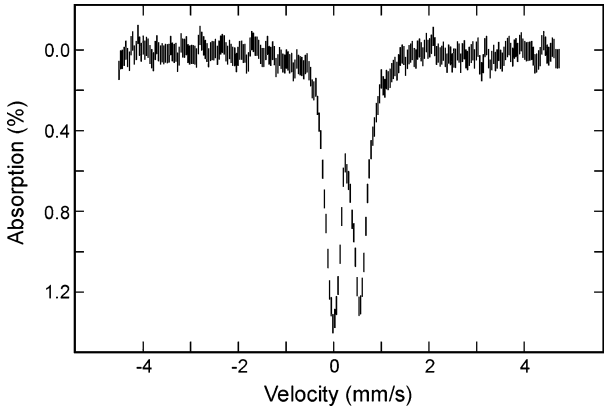

FIGURE 5: Mössbauer spectrum of a control sample of [2^{57}Fe−2S]/[4Fe−4S] BioB, which was incubated anearobically for 3.5 h in a solution identical to that used in the turnover experiment but without the presence of DTB. The spectrum was recorded at 4.2 K in a field of 50 mT oriented parallel to the γ-beam.

presented below, and it should not be taken literally that the degradation of the $[2Fe-2S]^{2+}$ cluster involves two independent exponential decays.

To correlate the degradation of the [2Fe−2S] cluster with the formation of biotin, we have performed the biotin assay on samples taken at the same time points during turnover (Materials and Methods). The results are plotted in Figure 4 as squares. These data also cannot be simulated with a single-exponential function, and thus, eq 2 was used.

$$B(t) = B_1[1 - \exp(-k_1 t)] + B_2[1 - \exp(-k_2 t)] \quad (2)$$

The dashed line displayed in Figure 4 is a simulation of eq 2 with $B_1 = 0.22$ biotin/monomer, $B_2 = 0.63$ biotin/monomer, $k_1 = 0.012$ min^{-1}, and $k_2 = 0.001$ min^{-1}. Comparing these parameters with those obtained for the decay of the $[2Fe-2S]^{2+}$ cluster indicates clearly that the production of biotin does not parallel the degradation of the $[2Fe-2S]^{2+}$ cluster. Particularly, the initial decay rate of the [2Fe−2S] cluster is about 1 order of magnitude faster than the initial formation rate of biotin.

Effects of DTB on the Stability of the [2Fe−2S] Cluster. To examine whether the stability of the [2Fe−2S] cluster is affected by the presence of DTB, we have performed a control experiment in which $[2^{57}Fe-2S]^{2+}$/$[4Fe-4S]^{2+}$ BioB was incubated anaerobically at 25 °C for 3.5 h in a solution identical to that of the turnover experiments except that DTB was not present. Figure 5 shows the Mössbauer spectrum of such a sample recorded at 4.2 K in a parallel field of 50 mT. The spectrum is very similar to that of the as-prepared [2^{57}Fe−2S]/[4Fe−4S] BioB (Figure 1A) and can be similarly decomposed into two components: a major quadrupole doublet accounting for ∼90% of the Fe absorption arising from the $[2Fe-2S]^{2+}$ cluster and a minor doublet (∼10%) that resembles the spectrum of a SAM-bound $[4Fe-4S]^{2+}$ cluster. The percent absorptions determined for the two clusters in the as-prepared and control [2^{57}Fe−2S]/[4Fe−4S] BioB samples are practically identical, indicating that the $[2Fe-2S]^{2+}$ cluster is stable in the absence of DTB. This observation, together with the results obtained from the turnover experiments, establishes that DTB is definitely involved in the degradation of the $[2Fe-2S]^{2+}$ cluster during turnover.

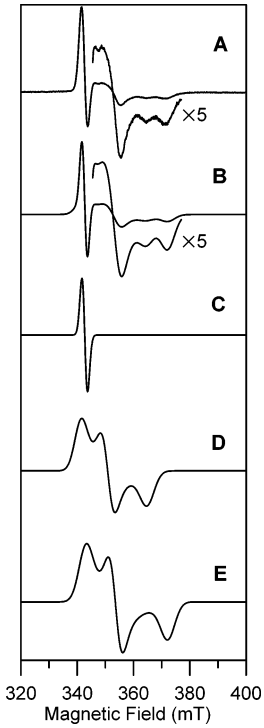

FIGURE 6: EPR spectrum of a natural abundance [2Fe−2S]/[4Fe−4S] BioB sample (200 μM) taken at 15 min reaction time during the single turnover reaction of the enzyme (A). Conditions of measurement were microwave frequency, 9.603 GHz; modulation amplitude, 0.63 mT; microwave power, 1 mW; temperature, 12 K. Panel B is a simulation of the spectrum in panel A as the sum of the three components: 7.6% of $g_{x,y,z} = 2.0015, 2.0015, 2.0018$ and $\Gamma_{x,y,z} = 2.0, 2.0, 2.0$ mT (C); 28.7% of $g_{x,y,z} = 1.880, 1.955, 2.010$ and $\Gamma_{x,y,z} = 5.0, 4.0, 4.5$ mT (D); 63.7% of $g_{x,y,z} = 1.845, 1.940, 2.000$ and $\Gamma_{x,y,z} = 5.0, 4.0, 5.0$ mT (E).

EPR Signals Observed during Single Turnover of [2Fe−2S]/[4Fe−4S] BioB. To further characterize the paramagnetic species generated during turnover, parallel EPR experiments were carried out using natural abundance [2Fe−2S]/[4Fe−4S] BioB (4.4 Fe/monomer) prepared with conditions identical to those used in the Mössbauer studies reported above. A transient EPR resonance was observed with maximum intensity in samples frozen after 15 min, see Figure 6A. This spectrum was simulated as a superposition of three EPR signals in Figure 6B: an isotropic radical signal at $g = 2.002$ (Figure 6C), which accounts for 7.5% of the total EPR absorption; an anisotropic $S = {}^1/_2$ resonance with $g = 2.01$, 1.96, and 1.88 corresponding to 28.5% of the total EPR absorption (Figure 6D); and an anisotropic $S = {}^1/_2$ resonance with $g = 2.00$, 1.94, and 1.85 corresponding to 64% of the total EPR absorption. The radical signal is attributed to the reducing system (NADPH/flavodoxin/flavodoxin reductase), since it was observed with similar intensity in all turnover samples (0 min to 24 h) and in control samples that did not contain BioB. The *g*-values of the two anisotropic resonances are indicative of $S = {}^1/_2$ Fe−S clusters but unambiguous simulation of the two is difficult because the low-field components are obscured by the radical signal. However, the assignment of the low-field components is in part based on the similarity to the EPR resonance reported by Jarrett and co-workers in samples of [2Fe−2S]/[4Fe−4S] BioB frozen under turnover conditions in the presence of $FeCl_3$, Na_2S, and DTT (*13*). These workers observed a broad, anisotropic, rhombic resonance, $g \approx 2.00$, 1.95, and 1.85,

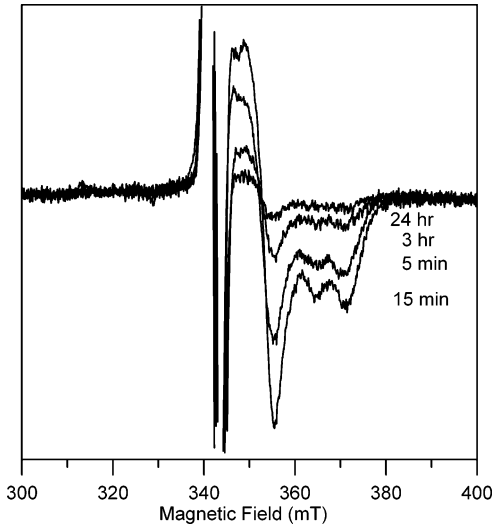

FIGURE 7: EPR spectra of a natural abundance [2Fe−2S]/[4Fe−4S] BioB sample (200 μM) taken at the indicated time periods during the single turnover reaction of the enzyme. Conditions of measurement were microwave frequency, 9.603 GHz; modulation amplitude, 0.63 mT; microwave power, 2 mW; temperature, 35 K.

without contributions from a radical species, that progressively increased during turnover in the presence of exogenous ferric iron at a rate comparable with biotin formation. This resonance was erroneously assigned to a $[3Fe-4S]^+$ cluster based on partial loss of intensity on addition of dithionite and the two low-field *g*-values (*13*). However, a temperature-dependent investigation indicates that these Fe−S cluster signals can be observed up to 70 K without significant broadening. Such temperature dependence behavior is typical for $S = {}^1/_2$ $[2Fe-2S]^+$ clusters and is inconsistent with assignment to either $S = {}^1/_2$ $[3Fe-4S]^+$ or $[4Fe-4S]^+$ clusters. Also, as presented above, the $[2Fe-2S]^+$ assignment is consistent with the overall magnetic hyperfine splitting of the paramagnetic species detected in the Mössbauer spectra.

The transient nature of the $[2Fe-2S]^+$ EPR signals observed during a single turnover of BioB is illustrated by the EPR spectra of samples taken at 5 min, 15 min, 3 h, and 24 h shown in Figure 7. After subtraction of the radical signal, spin quantitation of the two anisotropic resonances attributed to $[2Fe-2S]^+$ clusters under nonsaturating conditions (50 K and 1 mW) together accounts for 0.20, 0.31, 0.08, and 0.03 spins/BioB monomer in the 5-min, 15-min, 3-h and 24-h samples, respectively. The relative contributions of the two distinct resonances do not change significantly, suggesting that they correspond to conformational substates of the same $[2Fe-2S]^+$ cluster intermediate, rather than sequential $[2Fe-2S]^+$ cluster intermediates in the $[2Fe-2S]^{2+}$ cluster degradation pathway. Quantitatively analogous EPR results at equivalent reaction times were obtained for the turnover samples of $[2^{57}Fe-2S]/[4Fe-4S]$ and $[2^{57}Fe-2S]/[4^{57}Fe-4S]$ BioB used in the Mössbauer turnover experiments discussed above. Hence the EPR and Mössbauer quantitations concur in finding ~0.2 $[2Fe-2S]^+$ clusters per BioB monomer in the 5-min sample of $[2^{57}Fe-2S]/[4Fe-4S]$ BioB. Further, the EPR data support the assumption that the lower than expected Mössbauer absorption of the $[2^{57}Fe-2S]^{2+}$ signal in the $[2^{57}Fe-2S]/[4^{57}Fe-4S]$ BioB samples is a consequence of inefficient ^{57}Fe enrichment during growth. In summary, the EPR data clearly demonstrate that a $[2Fe-2S]^+$ cluster is formed as a transient intermediate in the rapid initial stage of $[2Fe-2S]^{2+}$ cluster degradation during turnover of [2Fe−2S]/[4Fe−4S] BioB.

DISCUSSION

We have used Mössbauer and EPR spectroscopy to monitor the time evolution of the Fe−S clusters in [2Fe−2S]/[4Fe−4S] BioB during turnover. The results indicate that under turnover conditions the [4Fe−4S] cluster is stable and present in a form that is similar to the SAM-bound $[4Fe-4S]^{2+}$ state reported previously for BioB containing only the [4Fe−4S] cluster (*26*). Spectroscopic evidence presented in our earlier study indicates that SAM binds to the $[4Fe-4S]^{2+}$ cluster at a unique Fe site (*26*). Binding of SAM to a unique Fe site of a $[4Fe-4S]^{2+}$ cluster has also been observed previously in a radical SAM enzyme, pyruvate formate-lyase activating enzyme (*27*−*29*), and is considered to be a common and functionally important property shared by radical SAM enzymes. Our observation thus supports the current consensus that BioB belongs to the family of radical SAM enzymes and suggests that the functional role of the [4Fe−4S] cluster in BioB is to bind SAM and facilitate the reductive cleavage that generates the catalytically important adenosyl radical. The fact that the $[4Fe-4S]^{2+}$ cluster is present in the SAM-bound form under turnover conditions suggests further that the immediate step following SAM binding, that is, the injection of an electron to the [4Fe−4S] cluster, must be the rate-limiting step in the reaction pathway involving the [4Fe−4S] cluster.

The changes occurring to the [2Fe−2S] cluster during turnover were also observed by our Mössbauer and EPR measurements, which show clearly that approximately ${}^2/_3$ of the [2Fe−2S] clusters were degraded by the end of the turnover experiment (24 h) with about half of the $[2Fe-2S]^{2+}$ clusters degraded within the first hour. Transient paramagnetic species, which exhibit spectroscopic properties that are indicative of $[2Fe-2S]^+$ clusters, were detected by both EPR and Mössbauer measurements, strongly suggesting that degradation of the $[2Fe-2S]^{2+}$ cluster is initiated by reduction of the cluster.

Degradation of the $[2Fe-2S]^{2+}$ cluster during [2Fe−2S]/[4Fe−4S] BioB turnover was initially reported by Jarrett and co-workers, who used UV/visible absorption spectroscopy to investigate changes occurring at or to the Fe−S clusters during catalysis (*13*). The decrease in absorbance at 460 nm was used as a quantitative measure of $[2Fe-2S]^{2+}$ degradation and was found to parallel the production of biotin, both in rate and in stoichiometry. On the basis of this UV/visible absorption data, together with Fe and S analysis, which showed a decrease in Fe and S contents consistent with loss of one [2Fe−2S] cluster per BioB, it was concluded that during catalysis the [4Fe−4S] cluster is preserved while the [2Fe−2S] cluster is destroyed. A mechanistic scheme consistent with such a conclusion was therefore proposed, in which the [4Fe−4S] cluster mediates the cleavage of SAM to generate an adenosyl radical that abstracts the C9 hydrogen atom of DTB to form a DTB radical, which, in turn, attacks a bridging sulfide of the $[2Fe-2S]^{2+}$ cluster initiating the destruction of the $[2Fe-2S]^{2+}$ cluster. A second adenosyl radical generated via the [4Fe−4S] cluster then abstracts the

C6 hydrogen atom followed by ring closure and formation of biotin. For the formation of biotin to parallel the destruction of the $[2Fe-2S]^{2+}$ cluster, the rate-limiting step in the proposed mechanism must correspond to [2Fe−2S] cluster degradation or a step preceding initiation of [2Fe−2S] cluster degradation. The Mössbauer and EPR data presented here are in general agreement with the conclusion made by Ugulava et al. (*13*) and provide direct evidence establishing that the [4Fe−4S] cluster is indeed preserved and that the $[2Fe-2S]^{2+}$ cluster is degraded during catalysis. However, the degradation of the $[2Fe-2S]^{2+}$ cluster was found not to parallel the formation of biotin, neither in rate nor in stoichiometry. Approximately half of the $[2Fe-2S]^{2+}$ clusters decay initially with a rate that is about 1 order of magnitude faster than that of the initial production of biotin. After 24 h, 0.7 biotin per BioB monomer was produced while only 0.5 $[2Fe-2S]^{2+}$ clusters per BioB monomer were destroyed, leaving approximately 0.25 $[2Fe-2S]^{2+}$ clusters per BioB monomer still intact. However, taking into consideration the estimated error in the biotin bioassay (0.7 ± 0.1 biotin per BioB monomer), and the possibility that some $[2Fe-2S]^{2+}$ clusters are reassembled under turnover conditions, the small difference in stoichiometry between biotin production and cluster destruction is unlikely to be significant.

Marquet and co-workers (*14*) have recently applied Mössbauer spectroscopy to investigate the states of the Fe−S clusters after catalysis in a partially purified fraction of BioB presumably having a 1:1 $[2Fe-2S]^{2+}/[4Fe-4S]^{2+}$ ratio. Since the protein fractions were partially purified, Fe content, and thus cluster content, per BioB monomer could not be obtained. Only the Mössbauer absorption ratio for the $[2Fe-2S]^{2+}$ and $[4Fe-4S]^{2+}$ could be determined. Their data also indicate that not all the $[2Fe-2S]^{2+}$ clusters are destroyed after turnover (37 °C for 3 h). Assuming that the $[4Fe-4S]^{2+}$ cluster is preserved after catalysis, the cluster absorption ratio determined by Marquet and co-workers indicates that approximately half of the [2Fe−2S] clusters remain intact, in good agreement with the results reported here.

In the scheme proposed by Ugulava et al. (*13*), the [2Fe−2S] cluster functions as the immediate sulfur donor for biotin production and the destruction of the $[2Fe-2S]^{2+}$ cluster begins with an attack of the bridging sulfide by a DTB radical. To investigate the involvement of DTB in the destruction of the [2Fe−2S] cluster, we have performed a control experiment in which DTB is left out of the turnover solution. In the absence of DTB, we found that the [2Fe−2S] cluster is stable for at least 3 h, by which time more than half of the $[2Fe-2S]^{2+}$ clusters had been degraded under turnover conditions. Consequently, DTB must be involved in the destruction of the cluster. Taken together, the involvement of DTB in the destruction of the [2Fe−2S] cluster and the observed decay of the $[2Fe-2S]^{2+}$ cluster during biotin production support the scheme proposed by Ugulava et al. (*13*). Since putative catalytic intermediates (the 6- or 9-thio derivatives of DTB) are not significantly active in the biotin bioassay (*30*), the observation that the initial rate of $[2Fe-2S]^{2+}$ cluster degradation is an order of magnitude faster than that of biotin formation can be explained by invoking a subsequent step in biotin synthesis, for example, the ring closure, to be the rate-limiting step. Alternatively, it is possible that a cluster degradation product, rather than the [2Fe−2S] cluster itself, is the immediate S donor. The degradation of the [2Fe−2S] cluster may generate protein-bound polysulfide or persulfide groups, which, in turn, serve as the immediate sulfur source for biotin production. Generation of protein-bound polysulfide groups following Fe−S cluster degradation is well established in at least one Fe−S enzyme, aconitase (*31*). This alternative explanation, which suggests a protein-bound persulfide or polysulfide group to be the S donor for biotin production, raises a rather interesting possibility concerning the active form of BioB. That is, the catalytically functional form of BioB may contain only a [4Fe−4S] cluster in addition to an active polysulfide or persulfide entity (i.e., the presence of a [2Fe−2S] cluster may not be required). Reactivation of such an active form of BioB after each single turnover would then involve regeneration of the active polysulfide or persulfide group rather than the reassembly of a [2Fe−2S] cluster as proposed for the [4Fe−4S]/[2Fe−2S] BioB. In the preceding paper (*4*), we have shown that, in our hands, BioB does not exhibit an intrinsic cysteine desulfurase activity. Therefore, regeneration of the active polysulfide or persulfide group in BioB would require an additional enzyme, such as a cysteine desulfurase possibly coupled with a specific sulfurtransferase as in the thiamin and 4-thiouridine biosynthetic pathways (*32*−*34*). Experiments are planned to investigate the validity of this rather intriguing possibility.

REFERENCES

1. Sanyal, I., Cohen, G., and Flint, D. H. (1994) Biotin synthase: purification, characterization as a [2Fe−2S] cluster protein, and in vitro activity of the *Escherichia coli* bioB gene product, *Biochemistry 33*, 3625−3631.
2. Duin, E. C., Lafferty, M. E., Crouse, B. R., Allen, R. M., Sanyal, I., Flint, D. H., and Johnson, M. K. (1997) [2Fe−2S] to [4Fe−4S] cluster conversion in *Escherichia coli* biotin synthase, *Biochemistry 36*, 11811−11820.
3. Tse Sum Bui, B., Florentin, D., Marquet, A., Benda, R., and Trautwein, A. X. (1999) Mössbauer studies of *Escherichia coli* biotin synthase: evidence for reversible interconversion between $[2Fe-2S]^{2+}$ and $[4Fe-4S]^{2+}$ clusters, *FEBS Lett. 459*, 411−414.
4. Cosper, M. M., Jameson, G. N. L., Hernández, H. L., Krebs, C., Huynh, B. H., and Johnson, M. K. (2004) Characterization of the cofactor composition of *Escherichia coli* biotin synthase, *Biochemistry 43*, 2007−2021.
5. Mejean, A., Tse Sum Bui, B., Florentin, D., Ploux, O., Izumi, Y., and Marquet, A. (1995) Highly purified biotin synthase can transform dethiobiotin into biotin in the absence of any other protein, in the presence of photoreduced deazaflavin, *Biochem. Biophys. Res. Commun. 217*, 1231−1237.
6. Baldet, P., Alban, C., and Douce, R. (1997) Biotin synthesis in higher plants: purification and characterization of *bioB* gene product equivalent from *Arabidopsis thaliana* overexpressed in *Escherichia coli* and its subcellular localization in pea leaf cells, *FEBS Lett. 419*, 206−210.
7. Sofia, H. J., Chen, G., Hetzler, B. G., Reyes-Spindola, J. F., and Miller, N. E. (2001) Radical SAM, a novel protein superfamily linking unresolved steps in familiar biosynthetic pathways with radical mechanisms: functional characterization using new analysis and information visualization methods, *Nucleic Acids Res. 29*, 1097−1106.
8. Escalettes, F., Florentin, D., Tse Sum Bui, B., Lesage, D., and Marquet, A. (1999) Biotin synthase mechanism: evidence for hydrogen transfer from the substrate into deoxyadenosine, *J. Am. Chem. Soc. 121*, 3571−3578.
9. Ugulava, N. B., Gibney, B. R., and Jarrett, J. T. (2000) Iron−sulfur cluster interconversions in biotin synthase: dissociation and reassociation of iron during conversion of [2Fe−2S] to [4Fe−4S] clusters, *Biochemistry 39*, 5206−5214.
10. Ollagnier-de Choudens, S., Sanakis, Y., Hewitson, K. S., Roach, P., Baldwin, J. E., Münck, E., and Fontecave, M. (2000) Iron−

sulfur center of biotin synthase and lipoate synthase, *Biochemistry 39*, 4165−4173.
11. Ugulava, N. B., Gibney, B. R., and Jarrett, J. T. (2001) Biotin synthase contains two distinct iron−sulfur cluster binding sites: chemical and spectroelectrochemical analysis of iron−sulfur cluster interconversions, *Biochemistry 40*, 8343−8351.
12. Ugulava, N. B., Surerus, K. K., and Jarrett, J. T. (2002) Evidence from Mössbauer spectroscopy for distinct $[2Fe-2S]^{2+}$ and $[4Fe-4S]^{2+}$ cluster binding sites in biotin synthase from *Escherichia coli*, *J. Am. Chem. Soc. 124*, 9050−9051.
13. Ugulava, N. B., Sacanell, C. J., and Jarrett, J. T. (2001) Spectroscopic changes during a single turnover of biotin synthase: destruction of a [2Fe−2S] cluster accompanies sulfur insertion, *Biochemistry 40*, 8352−8358.
14. Tse Sum Biu, B., Brenda, R., Schünemann, V., Florentin, D., Trautwein, A. X., and Marquet, A. (2003) Fate of the $[2Fe-2S]^{2+}$ cluster of *Escherichia coli* biotin synthase during reaction: A Mössbauer characterization, *Biochemistry 42*, 8791−8798.
15. Ollagnier-de-Choudens, S., Mullier, E., Hewitson, K. S., and Fontecave, M. (2002) Biotin synthase is a pyridoxal phosphate-dependent cysteine desulfurase, *Biochemistry 41*, 9145−9152.
16. Hewitson, K. S., Ollagnier-de-Choudens, S., Sanakis, Y., Shaw, N. M., Baldwin, J. E., Münck, E., Roach, P. L., and Fontecave, M. (2002) The iron−sulfur center of biotin synthase: site-directed mutants, *J. Biol. Inorg. Chem. 7*, 83−93.
17. Ollagnier-de-Choudens, S., Sanakis, Y., Hewitson, K. S., Roach, P., Münck, E., and Fontecave, M. (2002) Reductive cleavage of *S*-adenosylmethionine by biotin synthase from *Escherichia coli*, *J. Biol. Chem. 277*, 13449−13454.
18. Cosper, M. M., Jameson, G. N. L., Eidsness, M. K., Huynh, B. H., and Johnson, M. K. (2002) Recombinant *Escherichia coli* biotin synthase is a $[2Fe-2S]^{2+}$ protein in whole cells, *FEBS Lett. 529*, 332−336.
19. Sanyal, I., Gibson, K. J., and Flint, D. H. (1996) *Escherichia coli* biotin synthase: an investigation into the factors required for its activity and its sulfur donor, *Arch. Biochem. Biophys. 326*, 48−56.
20. Gibson, K. J., Pelletier, D. A., and Turner, I. M. (1999) Transfer of sulfur to biotin from biotin synthase (BioB protein), *Biochem. Biophys. Res. Commun. 254*, 632−635.
21. Tse Sum Bui, B., and Marquet, A. (1997) Biotin synthase of *Bacillus sphaericus*, *Methods Enzymol. 279*, 356−362.
22. Tanaka, M., Izumi, Y., and Yamada, H. (1987) Biotin assay using lyophilized and glycerol-suspended cultures, *J. Microbiol. Methods 6*, 237−246.
23. Fish, W. W. (1998) Rapid colorimetric micromethod for the quantitation of complexed iron in biological samples, *Methods Enzymol. 158*, 357−364.
24. Ravi, N., Bollinger, J. M., Jr., Huynh, B. H., Stubbe, J., and Edmondson, D. E. (1994) Mechanism of assembly of the tyrosyl radical-diiron(III) cofactor of *E. coli* ribonucleotide reductase: 1. Mössbauer characterization of the diferric radical precursor, *J. Am. Chem. Soc. 116*, 8007−8014.
25. Dunham, W. R., Bearden, A. J., Salmeen, I. T., Palmer, G., Sands, R. H., Orme-Johnson, W. H., and Beinert, H. (1971) Electronic properties of two-iron, two-sulfur proteins. II. Two-iron ferredoxins in spinach, parsley, pig adrenal cortex, *Azotobacter vinelandii*, and *Clostridium pasteurianum*. Magnetic field Mössbauer spectroscopy, *Biochim. Biophys. Acta 253*, 134−152.
26. Cosper, M. M., Jameson, G. N. L., Davydov, R., Eidsness, M. K., Hoffman, B. M., Huynh, B. H., and Johnson, M. K. (2002) The $[4Fe-4S]^{2+}$ cluster in reconstituted biotin synthase binds *S*-adenosyl-L-methionine, *J. Am. Chem. Soc. 124*, 14006−14007.
27. Krebs, C., Broderick, W. E., Henshaw, T. F., Broderick, J. B., and Huynh, B. H. (2002) Coordination of adenosylmethionine to a unique iron site of the [4Fe−4S] of pyruvate formate-lyase activating enzyme: a Mössbauer spectroscopic study, *J. Am. Chem. Soc. 124*, 912−913.
28. Walsby, C. J., Ortillo, D., Broderick, W. E., Broderick, J. B., and Hoffman, B. M. (2002) An anchoring role for FeS clusters: Chelation of the amino acid moiety of *S*-adenosylmethionine to the unique iron site of the [4Fe−4S] cluster of pyruvate formate-lyase activating enzyme, *J. Am. Chem. Soc. 124*, 11270−11271.
29. Walsby, C. J., Hong, W., Broderick, W. E., Cheek, J., Ortillo, D., Broderick, J. B., and Hoffman, B. M. (2002) Electron-nuclear double resonance spectroscopic evidence that *S*-adenosylmethionine binds in contact with the catalytically active $[4Fe-4S]^{+}$ cluster of pyruvate formate-lyase activating enzyme, *J. Am. Chem. Soc. 124*, 3143−3151.
30. Marquet, A., Frappier, F., Guillerm, G., Azoulay, M., Florentin, D., and Tabet, J.-C. (1993) Biotin biosynthesis: synthesis and biological evaluation of the putative intermediate thiols, *J. Am. Chem. Soc. 115*, 2139−2145.
31. Kennedy, M. C., and Beinert, H. (1988) The state of cluster sulfhydryl and sulfide of aconitase during cluster interconversions and removal. A convenient preparation of apoenzyme, *J. Biol. Chem. 263*, 8194−8198.
32. Palenchar, P. M., Buck, C., J., Cheng, H., Larson, T. J., and Mueller, E. G. (2000) Evidence that ThiI, an enzyme shared between thiamin and 4-thiouridine biosynthesis, may be a sulfurtransferase that proceeds through a persulfide intermediate, *J. Biol. Chem. 275*, 8283−8286.
33. Kambampati, R., and Lauhon, C. T. (2000) Evidence for the transfer of sulfane sulfur from IscS to ThiI during in vitro biosynthesis of 4-thiouridine in *Escherichia coli* tRNA, *J. Biol. Chem. 275*, 10727−10730.
34. Mueller, E. G., Palenchar, P. M., and Buck, C., J. (2001) The role of the cysteine residues of ThiI in the generation of 4-thiouridine in tRNA, *J. Biol. Chem. 276*, 33588−33595.

BI035666V